**HEFAT2014**
**10th International Conference on Heat Transfer, Fluid Mechanics and Thermodynamics**
**14 – 16 July 2014**
**Orlando, Florida**

# INVESTIGATION OF THE EFFECTS OF LATE IGNITION TIME ON THE DOMESTIC HOT WATER (DHW) COMFORT OF A COMBI BOILER TYPE HEATING APPLIANCE

Atmaca A. U.*, Erek A., and Altay H. M.
*Author for correspondence
Department of Mechanical Engineering,
Dokuz Eylül University,
İzmir, 35397,
Turkey,
E-mail: ugurcan.atmaca@deu.edu.tr

## ABSTRACT

Natural gas combi boilers are one of the most common branches of the household goods used for space and domestic hot water (DHW) heating. Although most of the combi boilers in the market have reached considerably high space heating efficiency values via condensing technology, there is still a huge demand on increasing their DHW comfort level and efficiency. Broad definition of the comfort level in the combi boilers is the expectation of an end-user to have hot water in a very short time and without fluctuations. DHW expectancy differs from market to market, therefore resulting in wide product diversity and a challenging competition between the manufacturers. The present study has mainly focused on the investigation of one of the parameters which are particularly effective on the DHW comfort level. As the first step, 1D mathematical model is constructed for DHW function with the transient energy equations of the concerning components. The differential energy equations of the model are discretized implicitly with Finite Difference Scheme in order to solve them numerically in Matlab. Boundary and initial conditions are defined as closely as possible to the exact working conditions. Thermodynamic properties of the flue gas mixture and water are obtained via open source software Cantera [1]. Then, the numerical results are compared with the experimental data to validate the model. After obtaining a model for basic applications and rough results to estimate the behavior of an appliance, one of the software parameters affecting the comfort level of the end-users, late ignition time is investigated numerically.

## NOMENCLATURE

| | | |
|---|---|---|
| $\rho_g$ | [kg/m$^3$] | density of the flue gas |
| $\rho_{wt}$ | [kg/m$^3$] | density of the water |
| $\rho_w$ | [kg/m$^3$] | density of the HC wall |
| $c_{pg}$ | [J/kg.K] | specific heat of the flue gas, |
| $c_{pw}$ | [J/kg.K] | specific heat of the HC wall |
| $c_{pwt}$ | [J/kg.K] | specific heat of the water |
| $T_g$ | [˚C] | temperature of combustion gases |
| $T_{wt(1)}$ | [˚C] | temperature of CH water in the HC |
| $T_{wt(2)}$ | [˚C] | temperature of CH water in the PHE |
| $T_{wt(3)}$ | [˚C] | temperature of DHW in PHE |
| $T_{adia}$ | [˚C] | adiabatic flame temperature |
| $T_\infty$ | [˚C] | surrounding air temperature |
| $T_w$ | [˚C] | HC wall temperature, ˚C |
| $\dot{m}_{su(1)}$ | [kg/s] | mass flow rate of CH water in HC |
| $\dot{m}_{su(2)}$ | [kg/s] | mass flow rate of CH water in PHE (per channel) |
| $\dot{m}_{su(3)}$ | [kg/s] | mass flow rate of DHW in PHE (per channel) |
| $\dot{m}_g$ | [kg/s] | mass flow rate of flue gas |
| $A_{sa,g}$ | [m$^2$] | HC inner heat transfer area (from gas domain) |
| $A_{cs,g}$ | [m$^2$] | cross-sectional area through which flue gas flows |
| $A_{sa,wt(1)}$ | [m$^2$] | HC outer heat transfer area (to the CH water ) |
| $A_{cs,wt(1)}$ | [m$^2$] | cross-sectional area through which CH water around the HC flows |
| $A_o$ | [m$^2$] | outermost area of HC (contact area with the surrounding air) |
| $A_{cs,w}$ | [m$^2$] | HC wall cross-sectional area along y2 direction |
| $A_{PHE}$ | [m$^2$] | heat transfer area of one plate |
| $h_g$ | [W/m$^2$.K] | convective heat transfer coefficient of flue gas in the HC |
| $h_{wt(1)}$ | [W/m$^2$.K] | convective heat transfer coefficient of CH water in the HC |
| $h_{wt(2)}$ | [W/m$^2$.K] | convective heat transfer coefficient of CH water in PHE |
| $h_{wt(3)}$ | [W/m$^2$.K] | convective heat transfer coefficient of DHW water in PHE |
| $h_\infty$ | [W/m$^2$.K] | natural convection coefficient of surrounding air |
| $U_{wt(1)}$ | [W/m$^2$.K] | overall heat transfer coefficient between CH water and HC wall |
| $U_{PHE}$ | [W/m$^2$.K] | overall heat transfer coefficient between CH water and DHW in PHE |
| $U_g$ | [W/m$^2$.K] | overall heat transfer coefficient between flue gas and HC wall |
| $l_{PHE}$ | [m] | length of PHE |
| s | [m] | HC length |
| z | [m] | CH water flow length around HC |
| $k_w$ | [W/m.K] | thermal conductivity of HC wall |
| $\eta_{fin}$ | [-] | fin efficiency |

| | | |
|---|---|---|
| $R_{t,g-w}$ wall | [K/W] | total thermal resistance between flue gas and HC wall |
| $R_{t,wt(1)-w}$ wall | [K/W] | total thermal resistance between CH water and HC wall |
| $R_{t,PHE}$ in PHE | [K/W] | total thermal resistance between CH water and DHW in PHE |
| $R_0$ | [m] | inner radius of HC wall |
| $R_1$ | [m] | average of outer and inner radius of HC wall |
| $R_2$ | [m] | outer radius of HC wall |
| $R_3$ | [m] | outermost radius of HC |
| $Q_{CH}$ | [kJ] | energy transferred from CH water to DHW in PHE |
| $V_{CHWC}$ | [$m^3$] | volume of CH water per channel of PHE |
| $V_{DHWC}$ | [$m^3$] | volume of DHW per channel of PHE |
| n | [-] | total number of CVs |
| t | [s] | time |
| $t_{final}$ | [s] | final time |

Subscripts/Superscripts:

| | | |
|---|---|---|
| m | [-] | number of the CV under study |
| p/p+1 | [-] | present/previous time step |

Abbreviations:

| | |
|---|---|
| CH | central heating |
| DHW | domestic hot water |
| DCW | domestic cold water |
| PHE | plate heat exchanger |
| HC | heat cell |
| HE | heat exchanger |
| CV | control volume |
| CHWC | central heating water channel |
| DHWC | domestic hot water channel |
| BC | boundary condition |
| IC | initial condition |

## INTRODUCTION

Combi boilers are integrated space/water heating appliances and due to the availability of natural gas, they are very common. Although every market has their own specifications, there are also some common targets that all manufacturers are trying to approach high DHW comfort levels and efficiency values while declaring their appliances. For space heating function highly efficient appliances are available. However, performance of a combi boiler still can be improved in term of DHW function. The current research and development activities are primarily focusing on high comfort level and efficiency appliances to cover the gap in DHW function to be more competitive in the market.

This study only touches on the investigation of an important software parameter, late ignition time, which is very critical to the comfort level of a combi boiler. Firstly, a theoretical model is constructed and verified experimentally for DHW heating function. Then, via this model the effects of this critical parameter is tried to estimate on the DHW outlet temperature.

As shown in Figure 1, the most important components of an ordinary gas-fired combi boiler in addition to its control unit are: (i) a primary heat exchanger (HE); (ii) a secondary heat exchanger; (iii) a pump; and (iv) a diverter valve. The system water that is sent to the radiators for space heating and to the secondary heat exchanger for DHW heating is called as central heating (CH) water. The primary heat exchanger and the secondary heat exchanger heat up the CH water and the DHW, respectively. In space heating mode, CH water heated by the primary heat exchanger is sent to the radiators to warm up the surrounding air. When there is domestic hot water demand, i.e. in the DHW mode, the diverter valve changes its position so that the heated CH water in the HE flows through the secondary heat exchanger (instead of flowing to the radiators) to warm up the tap water (domestic cold water (DCW)) to produce DHW.

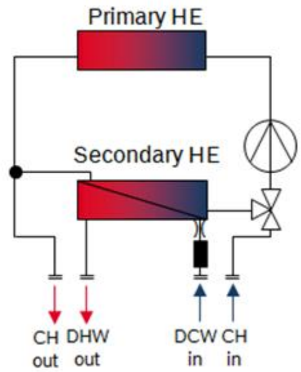


**Figure 1** Schematic view of a standard combi boiler

There are numerous academic researches similar to this heat exchanger modelling as summarized below. Bunce et al. [2] modelled a two-fluid counter-flow heat exchanger operating in steady state with constant inlet and outlet temperatures of the fluid streams. Junxiao et al. [3] created a lumped parameter model for a two-pass gas-to-gas cross-flow heat exchanger to investigate its transient behaviours. Ünal [4] modeled triple-concentric tube heat exchangers. Ataer et al. [5] proposed three different simulation techniques to predict the transient response of cross-flow, finned-type heat exchangers to step changes in the temperature of the entering fluid. Gut et al. [6] studied on the gasketed plate heat exchangers with generalized configurations to observe temperature profiles in all channels, the thermal effectiveness, the distribution of the overall heat transfer coefficient, and the pressure drop via a constructed mathematical model.

All researches are mainly about modelling a single heat exchanger under different operating conditions. Unlike to other studies, Atmaca et al. [7] proposed modelling of interconnected two heat exchangers in a combi boiler concept to simulate working conditions of integrated space/water heating appliances. Modelling coupling of two heat exchangers within the content of a heating appliance was also a promising step the cover the gap between comprehensive academic studies and real-life industrial problems for the benefits of the end-users. In that study, Atmaca et al. created a simple theoretical model including primary and secondary heat exchangers and validated the theoretical results with experiments at a specific flow rate corresponding constant power in the software of the appliance.

In this study, the theoretical model of the combi boiler has been explained and verified at a kind of lower flow rate resulting in power modulation according to the appliance working algorithm. Specifically, the impacts of late ignition time on DHW outlet temperature has been investigated on numerical basis to state some rough remarks on the comfort level of the appliance.

## COMPONENTS OF THE COMBI BOILERS

The primary heat exchanger as shown in Figure 2 is called heat cell (HC) and has combustion inside. As summarized before the energy of the hot combustion products is transferred to the system water (CH water) circulating around the HC.

Heat transfer area of the HC between the hot combustion products and the cold CH water is enlarged with numerous number of pin fins for maximum heat transition. In addition to fins, cross-flow arrangement of HC is also an important aspect for maximum heat transfer.

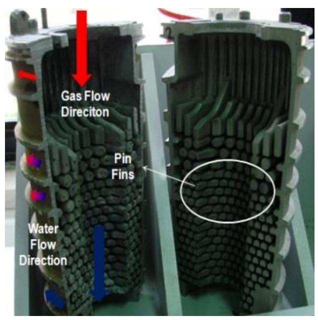


**Figure 2** Cross-sectional view of the modelled heat cell (Conical HC)

The secondary heat exchanger is plate heat exchanger as shown in Figure 3. It has a layer by layer structure and the forms of the plates are of main importance to the heat transfer characteristics. A PHE has so compact sizes that it occupies very little volume in a combi boiler. The number of the plates is dependent upon the power of the heating appliance. Corresponding PHE to the heat cell in the appliance concept under investigation has 24 plates and counter-flow arrangement.

**Figure 3** PHEs having different number of plates

For the primary heat exchanger, energy equations of the combustion products, HC wall, and the CH water around the HC have been constituted, whereas the energy equations of the CH water in PHE and DHW in PHE have been built-up for the secondary heat exchanger. It is required to solve five of these equations at the same time to create real appliance working simulations on the computer.

## ECO/COMFORT MODE IN A COMBI BOILER

There are two basic working modes in a combi boiler as eco and comfort mode in terms of DHW heating function. In eco mode, when tapping is created, the CH water and DHW is heated up instantaneously. However, in comfort mode, the CH water in the small circuit of HC and PHE is heated periodically to keep the water hot enough to decrease the waiting period when the users demand hot water. The critical temperature limits that the CH water is tried to kept between is shown in Figure 4 and the pre-heat periods differs from appliance to appliance. The experimental data was collected from an appliance operating in comfort mode when there was no hot water request.

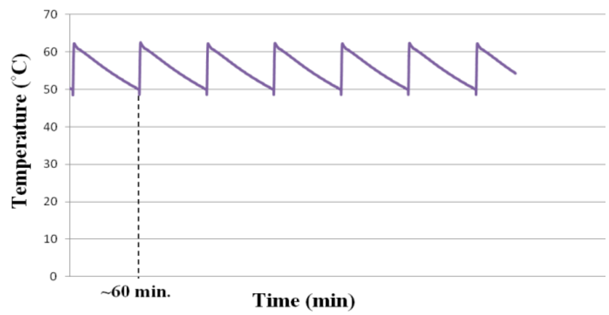


**Figure 4** Regular heating periods of CH water because of losses to the environment (no hot water demand)

Therefore DHW set temperature is reached rapidly as shown in Figure 5. Thanks to the pre-heat phases, DCW is heated up to the desired set temperature levels in a shorter time when compared to eco mode.

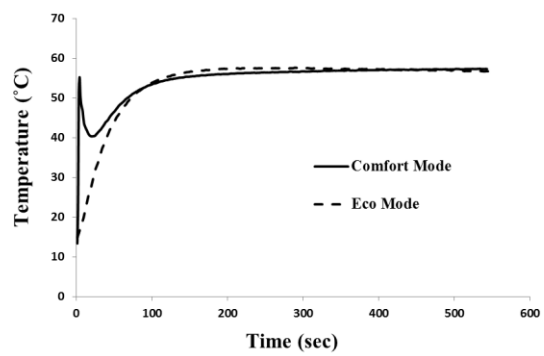


**Figure 5** Comparison of the experimental DHW outlet temperature in eco and comfort mode

The model has been validated both in eco and comfort mode working configuration. Eco mode simulations are including also power modulation at the requested DHW flow rate according to the appliance working algorithm.

## COMFORT TESTS OF THE COMBI BOILERS

An international test instruction is established in order to create a common decision mechanism about the comfort level of the gas-fired domestic appliances producing hot water (not exceeding 70 kW heat input and 300 l water storage capacity) [8]. There are 6 different tests for measuring the comfort level of a combi boiler type appliance in the content of the above mentioned test instruction. *"Waiting Time Test"* is the most important one because of being directly related to this study. In this test, DHW outlet temperature profile is investigated if a hot water demand is created after an appliance gets out of the comfort cycles where CH water is periodically heated in case of possible user requests. According to the minimum and maximum points of DHW outlet temperature and the time duration between these points, the appliance gets a score. Hence, the most important points of this test are the minimum and maximum points of DHW outlet temperature and the elapsed time between these maximum and minimum peaks. Since the CH water and the system components are hot, when DHW request is created, there is a direct increase in the DHW outlet temperature as also shown in Figure 5. According to the software of the appliance, if there is hot water inside, the appliance cannot start ignition directly at the time of DHW tapping. This period is called late ignition time. Because of the late ignition, both CH and DHW temperature decreases. After decreasing below a critical point defined for CH temperature, ignition starts causing to increase in DHW outlet temperature. As a result, the higher peak and the lower peak in Figure 5 are due to the heat retention and late ignition time, respectively.

In this study, the main objective is to estimate the effects of late ignition time on the DHW outlet temperature via the constructed model.

## THEORETICAL MODEL

A combi boiler has been modeled with the combination of the HC in Figure 2 and PHE in Figure 3. The assumptions used in the model are as flows:

- The transient energy equations are 1D.
  T=f(x, t)
- There are no thermal energy sources within the exchangers.
- Heat losses to the environment are taken into consideration for HC; whereas assumed negligible for PHE.
- The mass flow rates of both streams do not vary with time. Fluid passages are uniform in cross-sections.
- The velocity and temperature of each fluid at the inlet are uniform over the flow cross-section.
- The convective heat transfer coefficients on each side are constant.
- Thermal properties of the water are used as constant values although thermal properties of the flue gas and the wall changes with temperature.
- Longitudinal heat conduction within the fluids is neglected, but diffusion terms are added to the HC wall equation.
- The heat transfer surface area on each fluid side is uniformly distributed in the heat exchangers.
- The fouling resistance in PHE is negligible.
- Temperature profiles of CH water and DHW are same along each CH water channel and DHW channel, respectively.
- In PHE, thermal resistance of the plates considered negligible; but in HC, wall resistance is evaluated.

### 1D Transient Energy Equations

Working principle of a combi boiler and the interconnected BCs for the equations are summarized in Figure 6. Equations are obtained for (i) the flue gas, (ii) the CH water in HC, (iii) the HC wall, (iv) the CH water flowing through one layer of PHE, and (v) the DHW flowing through the subsequent layer of PHE.

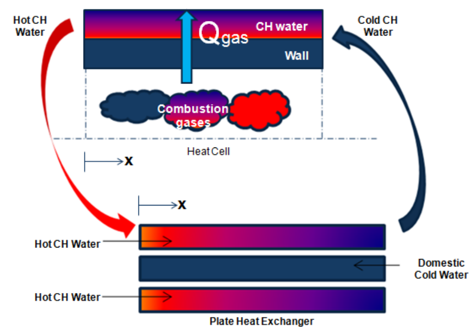


**Figure 6** Schematic display of working principle of a combi boiler

While deriving the governing differential equations, the control volumes (CVs) and flow directions are shown in Figure 7 for the HC [7].

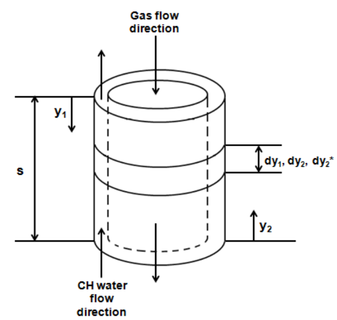


**Figure 7** Flow directions for the flue gas, HC wall, and the CH water in HC

For PHE model, CVs and flow directions of the CH water and DHW are shown in Figure 8 [7].

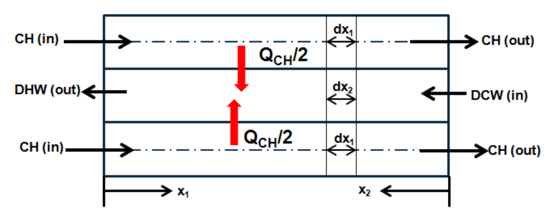


**Figure 8** Flow directions in PHE

The cooling of hot combustion gases in $y_1$ direction is expressed as

$$\rho_g A_{cs,g} c_{pg} \frac{\partial T_g}{\partial t} = -\dot{m}_g c_{pg} \frac{\partial T_g}{\partial y_1} - \frac{A_{sa,g} U_g}{s}(T_g - T_w) \qquad (1)$$

Total thermal resistances are also modeled for CH water and gas domain as it is shown in Figure 9 [9].

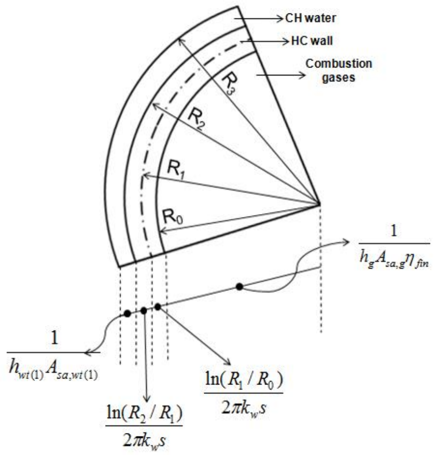


**Figure 9** Modelling of thermal resistances in the HC [9]

The total thermal resistance between the HC wall and the combustion gases is as follows:

$$R_{t,g-w} = \frac{1}{U_g A_{sa,g}} = \frac{1}{h_g A_{sa,g} \eta_{fin}} + \frac{\ln(R_1/R_0)}{2\pi k_w s} \tag{2}$$

The heating of CH water in the HC along $y_2$ direction is given by

$$\rho_{wt} A_{cs,wt(1)} c_{pwt} \frac{\partial T_{wt(1)}}{\partial t} = -\dot{m}_{wt(1)} c_{pwt} \frac{\partial T_{wt(1)}}{\partial y_2} + \frac{U_{wt(1)} A_{sa,wt(1)}}{z}(T_w - T_{wt(1)}) - h_\infty \frac{A_o}{z}(T_{wt(1)} - T_\infty) \tag{3}$$

The total thermal resistance between the HC wall and CH water is

$$R_{t,wt(1)-w} = \frac{1}{U_{wt(1)} A_{sa,wt(1)}} = \frac{1}{h_{wt(1)} A_{sa,wt(1)}} + \frac{\ln(R_2/R_1)}{2\pi k_w s} \tag{4}$$

The temperature distribution of the HC wall along $y_2$ direction is explained by

$$\rho_w A_{cs,w} c_w \frac{\partial T_w}{\partial t} = k_w \frac{\partial^2 T_w}{\partial y_2^2} A_{cs,w} + \frac{U_g A_{sa,g}}{s}(T_g - T_w) - \frac{U_{wt(1)} A_{sa,wt(1)}}{s}(T_w - T_{wt(1)}) \tag{5}$$

The temperature distribution of CH water in PHE along $x_1$ direction is expressed as

$$\rho_{wt} \frac{V_{CHWC}}{l_{PHE}} c_{pwt} \frac{\partial T_{wt(2)}}{\partial t} = -\dot{m}_{wt(2)} c_{pwt} \frac{\partial T_{wt(2)}}{\partial x_1} - 2\frac{U_{PHE} A_{PHE}}{l_{PHE}}(T_{wt(2)} - T_{wt(3)}) \tag{6}$$

The total thermal resistance in the PHE is written as follows:

$$R_{t,PHE} = \frac{1}{U_{PHE} A_{PHE}} = \frac{1}{h_{wt(2)} A_{PHE}} + \frac{1}{h_{wt(3)} A_{PHE}} \tag{7}$$

The heating of DCW in $x_2$ direction is calculated from

$$\rho_{wt} \frac{V_{DHWC}}{l_{PHE}} c_{pwt} \frac{\partial T_{wt(3)}}{\partial t} = -\dot{m}_{wt(3)} c_{pwt} \frac{\partial T_{wt(3)}}{\partial x_2} + 2\frac{U_{PHE} A_{PHE}}{l_{PHE}}(T_{wt(2)} - T_{wt(3)}) \tag{8}$$

**Discretisation of the Equations**

The above given differential equations have been discretised implicitly with Finite Difference Method to obtain numerical solutions. Implicit discretization of HC equations are done based on the control volume numbers shown as in Figure 10.

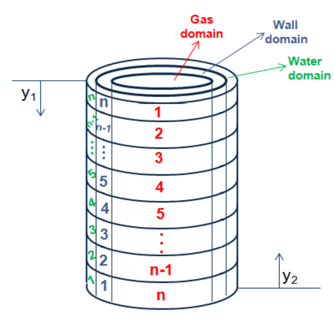


**Figure 10** Control volume numbers for the combustion gases, the CH water, and HC wall

CV numbers that are used to discretise the equations of CH water and DHW domains are given in Figure 11.

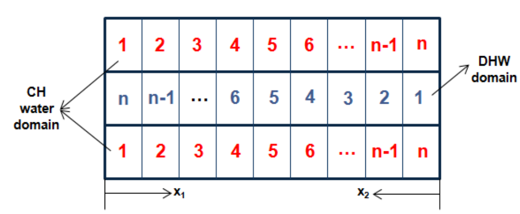


**Figure 11** Control volume numbers for the CH water and DHW channels of PHE

The discretised form of Equation (1) is

$$\rho_g A_{cs,g} c_{pg} \left(\frac{T_{g(m)}^{p+1} - T_{g(m)}^{p}}{dt}\right) = - \dot{m}_g\, c_{pg} \left(\frac{T_{g(m)}^{p+1} - T_{g(m-1)}^{p+1}}{dy_1}\right) - \frac{A_{sa,g} U_g}{s} \left(T_{g(m)}^{p+1} - T_{w((s/dy_1)-m+1)}^{p+1}\right) \tag{9}$$

The discretised version of Equation (3) is as follows

$$\rho_{wt} A_{cs,wt(1)} c_{pwt} \left(\frac{T_{wt(1)(m)}^{p+1} - T_{wt(1)(m)}^{p}}{dt}\right) = - \dot{m}_{wt(1)}\, c_{pwt} \left(\frac{T_{wt(1)(m)}^{p+1} - T_{wt(1)(m-1)}^{p+1}}{dy_2}\right) + \frac{U_{wt(1)} A_{sa,wt(1)}}{z} \left(T_{w(m)}^{p+1} - T_{wt(1)(m)}^{p+1}\right) - h_\infty \frac{A_o}{z} \left((T_{wt(1)(m)}^{p+1} - T_\infty\right) \tag{10}$$

The discretised form of Equation (5) is given by

$$\rho_w A_{cs,w} c_w \left(\frac{T_{w(m)}^{p+1} - T_{w(m)}^{p}}{dt}\right) = k_w A_{cs,w} \left(\frac{T_{w(m+1)}^{p+1} - 2T_{w(m)}^{p+1} + T_{w(m-1)}^{p+1}}{(dy_2{*})^2}\right) + \frac{U_g A_{sa,g}}{s} \left(T_{g((s/dy_1)-m+1)}^{p+1} - T_{w(m)}^{p+1}\right) - \frac{U_{wt(1)} A_{sa,wt(1)}}{s} \left(T_{w(m)}^{p+1} - T_{wt(1)(m)}^{p+1}\right) \tag{11}$$

The discretization of Equation (6) is expressed as

$$\rho_{wt} \frac{V_{CHWC}}{l_{PHE}} c_{pwt} \left(\frac{T_{wt(2)(m)}^{p+1} - T_{wt(2)(m)}^{p}}{dt}\right) = - \dot{m}_{wt(2)}\, c_{pwt} \left(\frac{T_{wt(2)(m)}^{p+1} - T_{wt(2)(m-1)}^{p+1}}{dx_1}\right) - 2 \frac{U_{PHE} A_{PHE}}{l_{PHE}} \left(T_{wt(2)(m)}^{p+1} - T_{wt(3)((l_{PHE}/dx_1)-m+1)}^{p+1}\right) \tag{12}$$

The descretised form of Equation (8) is

$$\rho_{wt} \frac{V_{DHWC}}{l_{PHE}} c_{pwt} \left(\frac{T_{wt(3)(m)}^{p+1} - T_{wt(3)(m)}^{p}}{dt}\right) = - \dot{m}_{wt(3)}\, c_{pwt} \left(\frac{T_{wt(3)(m)}^{p+1} - T_{wt(3)(m-1)}^{p+1}}{dx_2}\right) + 2 \frac{U_{PHE} A_{PHE}}{l_{PHE}} \left(T_{wt(2)((l_{PHE}/dx_1)-m+1)}^{p+1} - T_{wt(3)}^{p+1}\right) \tag{13}$$

It should be stated that although both the HC wall and the CH water equations are written in $y_2$ direction, $dy_2$ and $dy_2{*}$ are different from each other since the helical path of CH water around HC is longer than the HC length.

**Initial and Boundary Conditions**

After discretization has been completed, for constructing the numerical solution algorithm, the boundary and initial conditions (BCs & ICs) must be known. BCs are same for all calculations, but ICs are defined while taking the real working conditions of the appliances into consideration. The below ICs are for eco mode simulation.

Initial conditions for the HC wall, the CH water in HC and PHE, the flue gas and DHW are as follows

$$T_{g,wt(1),w}(y_{1,2},0) = 10\ °C \tag{14}$$

$$T_{wt(2),wt(3)}(x_{1,2},0) = 10\ °C \tag{15}$$

The BCs of the CH water in HC and in PHE are interconnected and dependent on time as explained by

$$T_{wt(1)}(0,t) = T_{wt(2)}((l_{PHE}/dx_1),t) \tag{16}$$

$$T_{wt(2)}(0,t) = T_{wt(1)}((z/dy_2),t) \tag{17}$$

The BCs of DCW and the flue gas are used as constant values and given by

$$T_{wt(3)}(0,t) = 10\ °C \tag{18}$$

$$T_g(0,t) = T_{adia} \tag{19}$$

All the equations except the HC wall are first order partial differential equations. Then, for wall two boundary conditions are defined as convection surface condition [9] by

$$-k_w \frac{\partial T_w}{\partial y_2}\Big|_{y_2=0} = h_\infty (T_\infty - T_w(0,t)) \tag{20}$$

$$-k_w \frac{\partial T_w}{\partial y_2}\Big|_{y_2=(s/dy_1)} = h_\infty (T_\infty - T_w((s/dy_1),t)) \tag{21}$$

## VALIDATION OF THE MODEL

The numerical model was validated with the experimental data as the next step. A special test rig (shown in Figure 12) which is manufactured for special efficiency and comfort tests was used for experimental verification. DHW inlet and outlet temperatures can be directly recorded.

However, the test rig doesn't record CH inlet and outlet temperatures from the HC. Then, thermocouples are attached externally for temperature measurement as shown in Figure 13.

**Figure 12** Special test rig for comfort and efficiency tests of combi boilers

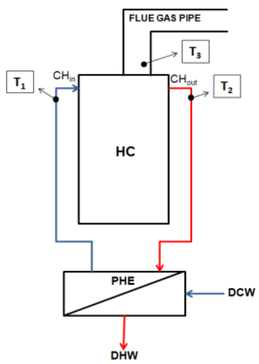


**Figure 13** Thermocouples attachment points for additional temperature measurements

Figure 14 shows the numerical and experimental CH water temperature of 24-plate PHE and the conical HC combination at the HC inlet in eco mode at 7 l/min DHW flow rate.

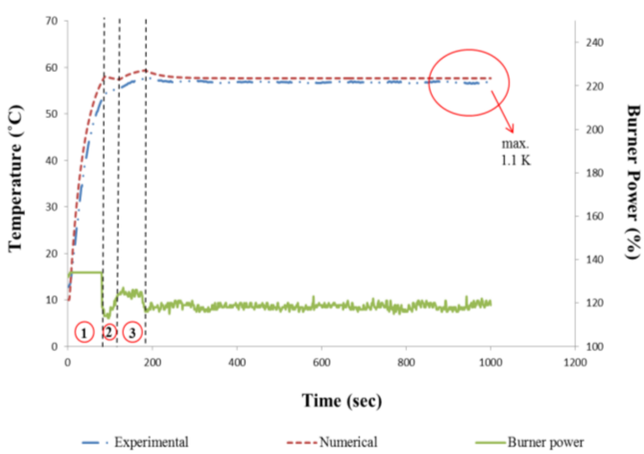


**Figure 14** Comparison between the numerical and experimental CH water temperature of 24-plate PHE and the conical HC combination at the HC inlet in eco mode at 7 l/min DHW flow rate

Figure 15 shows the numerical and experimental CH water temperature of 24-plate PHE and the conical HC combination at the HC outlet in eco mode at 7 l/min DHW flow rate.

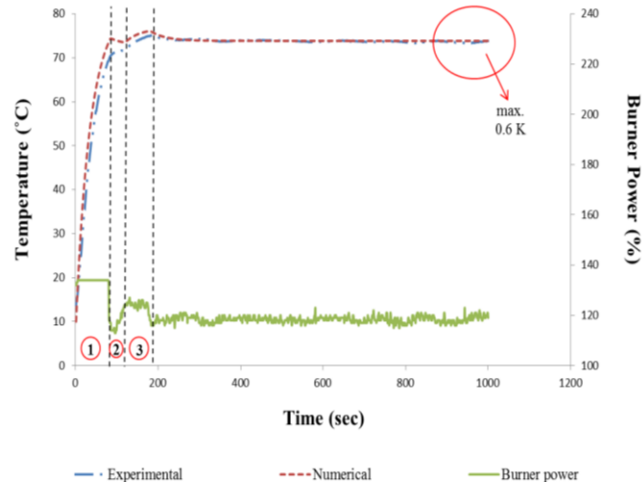


**Figure 15** Comparison between the numerical and experimental CH water temperature of 24-plate PHE and the conical HC combination at the HC outlet in eco mode at 7 l/min DHW flow rate

Figure 16 shows the numerical and experimental DHW outlet and inlet temperature difference of 24-plate PHE and the conical HC combination in eco mode at 7 l/min DHW flow rate.

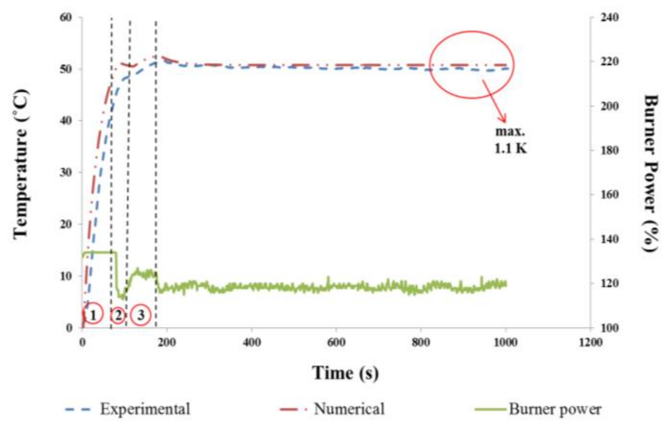


**Figure 16** Experimental and numerical DHW inlet and outlet temperature difference of the 24-plate PHE and the conical HC combination in eco mode at 7 l/min

Good agreement between the numerical and experimental results shows that the established model can be used to evaluate the effects of any parameter of the system.

## RESULTS AND DISCUSSION

After the numerical model is validated in eco mode, it is time to evaluate the closeness of the numerical and experimental data in comfort mode. As it is seen from Figure 5, there are two peaks in the DHW outlet temperature after creating tapping in comfort mode. The upper peak is due to the heat retention, whereas the lower peak is because of the late ignition time as it is described before. As a result, creating those conditions in the solution algorithm, both of the peaks will be observed in the numerical results.

Figure 17 shows the numerical and experimental DHW outlet and inlet temperature difference of 24-plate PHE and the conical HC combination in comfort mode at 7 l/min DHW flow rate.

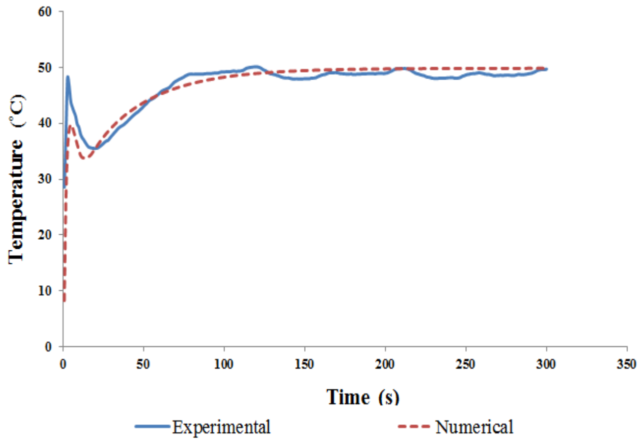


**Figure 17** Experimental and numerical DHW inlet and outlet temperature difference of the conical HC and 24-plate PHE combination in comfort mode at 7 l/min

The difference between the peaks shows us that the numerical results cannot be used directly for crucial decisions, for example to obtain the exact results of "Waiting Time Test" with numerical calculations. However, the system behaviour could be roughly estimated to decrease the test numbers, prototype costs, etc. With defining the sensitivity of the model, it can be stated that the comfort mode simulations could be created with this numerical model. Then the effects of one of the most important software parameter, late ignition time could be investigated on this numerical model as shown Figure 18.

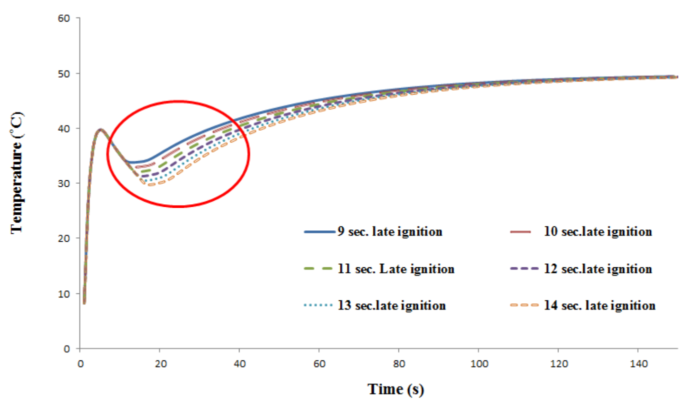


**Figure 18** The effects of late ignition time on the temperature difference between the DHW inlet and outlet at 7 l/min in comfort mode

Then, the numerical model helped us to estimate the effects of even 1 second late ignition in the DHW outlet temperature. With those kinds of trials, different software parameter changes also could be tried with the numerical model.

## CONCLUSION

Eco mode simulations with power modulation shows good agreement, but comfort mode simulations are to be improved.

The constructed model is 1D and based on too many assumptions, correlations, etc. Actually, the gas flow inside the HC should be modelled in detail with computational fluid dynamics. The exact values of the heat transfer coefficients could be estimated better in that way. Using general correlations isn't as safe as flow analyses or experimental approaches. Moreover, the heat transfer coefficients also changes locally. Due to the simplicity, our model lacks of those important details thereby resulting rough closeness between the experimental and numerical results in comfort mode.

The numerical results cannot be used in direct applications. Without the above mentioned improvements, the numerical model can just be used for comparison between the appliance concepts or for general estimations before going to laboratory for testing to decrease the number of the experiments and before producing prototypes to avoid excessive costs.

In conclusion, with these simulations, it will be possible to compare directly the effects of the system parameters on the appliances and calculate the results of the planned changes to have just a broad idea. In other words, by using such kind of model, trial-and-error phases, prototype costs, energy and time spent on the laboratory experiments of the changes on the regular appliances or completely new appliance designs are aimed to be decreased. Possible alternatives will be evaluated via simulations on the computers thereby resulting in less number of experiments or prototypes.

## ACKNOWLEDGEMENTS

This work has been funded by BOSCH TERMOTEKNİK ISITMA ve KLİMA SAN. TİC. A.Ş. We would like to convey our special thanks to them for their valuable financial and technical support.

## REFERENCES

[1] Goodwin D. G., Cantera: object-oriented software for reacting flows. Technical report. (http://www.cantera.org/).
[2] Bunce D.J., and Kandlikar S.G., 1995, "Transient Response of Heat Exchangers", Journal of Heat Transfer, Vol 119, 1995, pp. 729-736
[3] Junxiao S., Guiping L., Xiugan Y., Transient Performances of a Two-Pass Gas-to-Gas Crossflow Heat Exchanger, J. of Thermal Science, Vol 7, No. 1, 1998, pp. 67-70
[4] Ünal A., Theoretical Analysis of Triple Concentric-Tube Heat Exchangers, Part 1: Mathematical Modeling, Int. Comm. Heat Mass Transfer, Vol. 25, No. 7, 1998, pp. 949-958
[5] Atаer A.Ö., İleri A., Göğüş Y., Transient Behaviour of Finned-tube Cross-flow Heat Exchangers, Int. J. Refrig, Vol. 18, No. 3, 1995, pp. 153-160
[6] Gut J. A. W., Pinto J. M., Modeling of Plate Heat Exchangers with Generalized Configurations, International Journal of Heat and Mass Transfer 46 (2003) 2571-2585

[7] Atmaca, A. U., Altay, H. M., Ribeiro, B. A. R., Erek, A. (2013). Modeling of a dual function heating appliance for domestic hot water comfort. Recent Advances in Fluid Mechanics and Heat & Mass Transfer (Procedings of the 11. International Conference on Fluid Mechanics & Aerodynamics (FMA'13) and Procedings of the 11. International Conference on Heat Transfer, Thermal Engineering and Environment (HTE'13)), ISBN: 978-1-61804-183-8, 117-127.

[8] The European Standard EN 13203-1:2006, Gas-fired domestic appliances producing hot water- Appliances not exceeding 70 kW heat input and 300 l water storage capacity- Part 1: Assessment

[9] Incropera / DeWitt / Bergman / Lavine, Fundamentals of Heat and Mass Transfer, sixth edition, John Wiley & Sons, 2006